

Lorentz and CPT violation in the neutrino sector

V. Alan Kostelecký and Matthew Mewes

Physics Department, Indiana University, Bloomington, IN 47405, U.S.A.

(Dated: JUNE 14, 2003; accepted as a Rapid Communication, Phys. Rev. D)

We consider neutrino oscillations in the minimal Standard-Model Extension describing general Lorentz and CPT violation. Among the models without neutrino mass differences is one with two degrees of freedom that reproduces most major observed features of neutrino behavior.

Quantum physics and gravity are believed to combine at the Planck scale, $m_P \sim 10^{19}$ GeV. Experimentation at this high energy is impractical, but existing technology could detect suppressed effects from the Planck scale, such as violations of relativity through Lorentz or CPT breaking [1]. At experimentally accessible energies, signals for Lorentz and CPT violation are described by the Standard-Model Extension (SME) [2], an effective quantum field theory based on the Standard Model of particle physics. The SME incorporates general coordinate-independent Lorentz violation.

The character of the many experiments designed to study neutrino oscillations [3] makes them well suited for tests of Lorentz and CPT symmetry. The effects of Lorentz violation on propagation in the vacuum can become more pronounced for light particles, and so small effects may become observable for large baselines. Applying this idea to photons has led to the best current sensitivity on any type of relativity violation [4].

In this work, we study the general neutrino theory given by the minimal renormalizable SME [2]. In this setup, as in the usual minimal Standard Model, $SU(3) \times SU(2) \times U(1)$ symmetry is preserved, the right-handed neutrino fields decouple and so are unobservable, and there are no neutrino mass differences. The neutrino behavior is contained in the terms

$$L = \frac{1}{2} i \bar{L}_a \not{D} L_a + (a_L)_{ab} \bar{L}_a L_b + \frac{1}{2} i (c_L)_{ab} \bar{L}_a \not{D} L_b ; \quad (1)$$

where the first term is the usual Standard-Model kinetic term for the left-handed doublets L_a , with index a ranging over the three generations e, μ, τ . The coefficients for Lorentz violation are $(a_L)_{ab}$, which has mass dimension one and controls the CPT violation, and $(c_L)_{ab}$, which is dimensionless. It is attractive to view these coefficients as arising from spontaneous violation in a more fundamental theory [5], but other origins are possible [1].

The Lorentz-violating terms in Eq. (1) modify both interactions and propagation of neutrinos. Any interaction effects are expected to be tiny and well beyond existing sensitivities. In contrast, propagation effects can be substantial if the neutrinos travel large distances. The time evolution of neutrino states is controlled as usual by the effective hamiltonian $(h_e)_{ab}$ extracted from Eq. (1). The construction of $(h_e)_{ab}$ is complicated by the unconventional time-derivative term but can be performed

following the procedure in Ref. [6]. We find

$$(h_e)_{ab} = \not{p} j_{ab} + \frac{1}{\not{p} j} [(a_L)_{ab} \not{p} + (c_L)_{ab} \not{p} \not{p} L_{ab}] ; \quad (2)$$

To leading order, the 4-momentum p is $p = (\not{p} j, \not{p})$.

The analysis of neutrino mixing proceeds along the usual lines. We diagonalize $(h_e)_{ab}$ with a 3×3 unitary matrix U_e , $h_e = U_e^\dagger E_e U_e$, where E_e is a 3×3 diagonal matrix. There are therefore two energy-dependent eigenvalue differences and hence two independent oscillation lengths, as usual. The time evolution operator is $S_{ab}(t) = (U_e^\dagger e^{iE_{\text{eff}} t} U_e)_{ab}$, and the probability for a neutrino of type b to oscillate into a neutrino of type a in time t is $P_{b \rightarrow a}(t) = |S_{ab}(t)|^2$.

The CPT-conjugate hamiltonian h_e^{CPT} is obtained by changing the sign of a_L . Under CPT, the transition amplitudes transform as $S_{ab}(t) \rightarrow S_{ba}^*(t)$, so CPT invariance implies $P_{b \rightarrow a}(t) = P_{a \rightarrow b}(t)$. Note that the converse is false in general [7]. For instance, the model described below violates CPT but satisfies the equality.

Since oscillations are insensitive to terms proportional to the identity, each coefficient for Lorentz violation introduces two independent eigenvalue differences, three mixing angles, and three phases. The minimal SME (without neutrino masses) therefore contains a maximum of 160 gauge-invariant degrees of freedom describing neutrino oscillations [8]. Of these, 16 are rotationally invariant. The existing literature concerns almost exclusively the rotationally invariant case [9-12], usually with either a_L or c_L neglected and in a two-generation model with nonzero neutrino masses. A wealth of effects in the general case remains to be explored.

The presence of Lorentz violation introduces some novel features not present in the usual massive-neutrino case. One is an unusual energy dependence, which can be traced to the dimensionality of the coefficients for Lorentz violation. In the conventional case with mass-squared differences m^2 , neutrino oscillations are controlled by the dimensionless combination $m^2 L = E$ involving baseline distance L and energy E . In contrast, Eq. (2) shows that oscillations due to coefficients of type a_L and c_L are controlled by the dimensionless combinations $a_L L$ and $c_L L E$, respectively.

Another unconventional feature is direction-dependent dynamics, which is a consequence of rotational-symmetry violation. For terrestrial experiments, the direction dependence introduces sidereal variations in various observables at multiples of the Earth's sidereal frequency

$\theta = 23.5^\circ$ (23 h 56 m). For solar-neutrino experiments, it may yield annual variations because the propagation directions as the Earth orbits the Sun. Both types of variations offer a unique signal of Lorentz violation with interesting attainable sensitivities. For solar neutrinos $E \sim 10^{25}$, so a detailed analysis of existing data along the lines of Refs. [14] might achieve sensitivities as low as 10^{-28} GeV on a_L and 10^{-26} on c_L in certain models with Lorentz violation. These sensitivities would be comparable to the best existing ones in other sectors of the SME [4, 15[21].

The coefficients for Lorentz violation can also lead to novel resonances, in analogy to the MSW resonance [22]. Unlike the usual case, however, these Lorentz-violating resonances can occur also in the vacuum and may have directional dependence [23]. Note that conventional matter effects can readily be handled within our formalism (2) by adding the effective contributions $(a_{L,e})_{ee}^0 = \frac{G_F}{2} (2n_e - n_n)$ and $(a_{L,e})^0 = (a_{L,e})^0 = \frac{G_F}{2} n_n$, where n_e and n_n are the number densities of electrons and neutrons. The contributions to h_e from matter range from about 10^{-20} GeV to 10^{-25} GeV. This range is within the region expected for Planck-scale Lorentz violation, so matter effects can play a crucial role in the analysis.

An interesting question is whether the introduction of Lorentz violation may help explain the small LSND excess of $\bar{\nu}_e$ [24]. Usually, two mass-squared differences are invoked to explain the observations in solar and atmospheric neutrinos, but LSND lies well outside the region of limiting sensitivity to these effects. Possible solutions to this puzzle may arise from the unusual energy and directional dependences of Lorentz violation. An explanation of LSND requires a mass-squared difference of about 10^{-19} GeV $^2 = 10^{-1}$ eV 2 , an a_L of about 10^{-18} GeV, or a c_L of about 10^{-17} . Any of these would affect other experiments to some degree, including the MiniBooNE experiment [25] designed to test the LSND result.

To illustrate some of the possible behavior allowed by the SME, we consider a two-coefficient three-generation case without any mass-squared differences, but incorporating an isotropic c_L with nonzero element $\frac{4}{3}(c_L)_{ee}^{TT} = 2c$ and an anisotropic a_L with degenerate nonzero real elements $(a_L)_e^Z = (a_L)_e^Z = a = 2$. The coefficients are understood to be specified in the conventional Sun-centered celestial equatorial frame (T; X; Y; Z), which has Z axis along the Earth rotation axis and X axis towards the vernal equinox [13]. In what follows, we show that this simple model, which we call the 'bicycle' model, succeeds to reproduce the major features of the known neutrino behavior other than the LSND anomaly, despite having only two degrees of freedom rather than the four degrees of freedom used in the standard description with mass.

Diagonalizing the hamiltonian for the model yields

$$P_{ee} = 1 - 4 \sin^2 \theta \cos^2 \theta \sin^2(\theta_{31} L = 2);$$

$$P_{e\bar{e}} = P_{\bar{e}e} = 2 \sin^2 \theta \cos^2 \theta \sin^2(\theta_{31} L = 2);$$

$$\begin{aligned} P_{\mu\mu} &= P_{\mu\bar{\mu}} = 1 - \sin^2 \theta \sin^2(\theta_{21} L = 2) \\ &\quad - \sin^2 \theta \cos^2 \theta \sin^2(\theta_{31} L = 2) \\ &\quad - \cos^2 \theta \sin^2(\theta_{32} L = 2); \\ P_{\mu\bar{\mu}} &= \sin^2 \theta \sin^2(\theta_{21} L = 2) \\ &\quad - \sin^2 \theta \cos^2 \theta \sin^2(\theta_{31} L = 2) \\ &\quad + \cos^2 \theta \sin^2(\theta_{32} L = 2); \end{aligned} \quad (3)$$

where

$$\begin{aligned} p_{21} &= \frac{p}{(cE)^2 + (a \cos \theta)^2 + cE}; \\ p_{31} &= \frac{2p}{(cE)^2 + (a \cos \theta)^2}; \\ p_{32} &= \frac{p}{(cE)^2 + (a \cos \theta)^2 - cE}; \\ \sin^2 \theta &= \frac{1}{2} [1 - \frac{p}{cE} \frac{p}{(cE)^2 + (a \cos \theta)^2}]; \end{aligned} \quad (4)$$

and where we define the propagation direction by the unit vector $\hat{p} = (\sin \theta \cos \phi; \sin \theta \sin \phi; \cos \theta)$ in polar coordinates in the standard Sun-centered frame. These probabilities also hold for antineutrinos.

The qualitative features of the model can be understood as follows. At low energies, a causes oscillation of ν_e into an equal mixture of ν_μ and ν_τ . At high energies, c dominates and prevents ν_e mixing. For definiteness, we take $c > 0$. At energies well above the critical energy $E_0 = |a|/c$, $\sin^2 \theta$ vanishes and the probabilities reduce to a maximal mixing two-generation case with transition probability $P_{\mu\bar{\mu}} = \sin^2(\theta_{32} L = 2)$, $p_{32} = a^2 \cos^2 \theta = 2cE$. The energy dependence in this limit is therefore that of a conventional mass-squared difference of $m^2 = a^2 \cos^2 \theta = c$. This pseudomass appears because the hamiltonian contains one large element at high energies, triggering a Lorentz-violating seesaw. Other models using combinations of mass and coefficients for Lorentz violation can be constructed to yield various exotic E^n dependences at particular energy scales. Note that the high-energy pseudomass and hence neutrino oscillations depend on the declination of the propagation. High-energy neutrinos propagating parallel to celestial north or south experience the maximum pseudomass $m_0^2 = a^2 = c$, while others see a reduced value $m^2 = m_0^2 \cos^2 \theta$. For propagation in the equatorial plane, all off-diagonal terms in h_e vanish and there is no oscillation.

The features of atmospheric oscillations in the model are compatible with published observations. For definiteness, we take m_0^2 near the accepted range required in the usual analysis and E_0 below the relevant energies: $m_0^2 = 10^{-3}$ eV 2 and $E_0 = 0.1$ GeV ($c = 10^{-19}$, $a = 10^{-20}$ GeV). High-energy atmospheric neutrinos then exhibit the usual energy dependence, despite having zero mass differences. The zenith-angle dependence of the probability $P_{\mu\bar{\mu}}$ averaged over the azimuthal angle also is comparable within existing experimental resolution to a conventional maximal mixing case with two generations and a mass-squared difference $m^2 = 2 \times 10^{-3}$ eV 2 , as is shown in Fig. 1 for latitude $\theta = 36^\circ$. However, the model predicts significant azimuthal dependence for

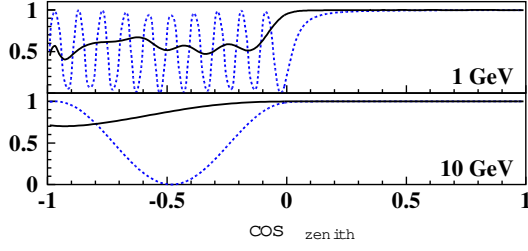


FIG. 1: $P_{e \rightarrow e}$ averaged over azimuthal angle for the bicycle model (solid) and for a conventional case with mass (dotted).

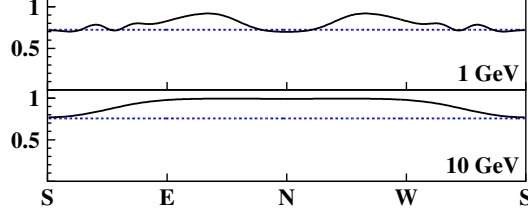


FIG. 2: $P_{e \rightarrow e}$ averaged over zenith angle for the bicycle model (solid) and for a conventional case with mass (dotted).

atmospheric neutrinos, which is a signal for Lorentz violation. For example, consider neutrinos propagating in the horizontal plane of the detector. Neutrinos originating from the east or west have $\cos \theta = 0$, $m^2 = 0$, and hence no oscillations. In contrast, those entering the detector from the north or south experience a pseudomass of $m^2 = m_0^2 \cos^2 \theta$. Figure 2 shows the survival probability averaged over zenith angle as a function of azimuthal angle. Although this model predicts no east-west asymmetry beyond the usual case, north-east or north-south asymmetries appear. Similar ‘compass’ asymmetries are typical in all direction-dependent models.

The basic features of solar-neutrino oscillations predicted by the model are also compatible with observation. Observed solar neutrinos propagate in the Earth’s orbital plane, which lies at an angle $\theta \approx 23^\circ$ relative to the equatorial plane. The value of $\cos^2 \theta$ therefore varies from zero at the two equinoxes to its maximum of $\sin^2 23^\circ$ at the two solstices. Assuming adiabatic propagation in the Sun, the average $e \rightarrow e$ survival probability is

$$(P_{e \rightarrow e})_{\text{adiabatic}} = \sin^2 \theta \sin^2 \theta_0 + \cos^2 \theta \cos^2 \theta_0; \quad (5)$$

where θ_0 is the mixing angle at the core, given by replacing $\mathcal{C}E$ with $\mathcal{C}E + G_F n_e = \bar{2}$ in Eq. (4). Figure 3 shows the adiabatic probability as a function of energy averaged over one year. The predicted neutrino flux is half the expected value at low energies and decreases at higher energies, consistent with existing data. Also shown is the adiabatic probability at approximately weekly intervals between an equinox and a solstice. Over much of the year, it remains near the average. There is a strong reduction near each equinox, but the adiabatic approximation fails there because oscillations cease, and so the true survival probability peaks sharply to unity. The

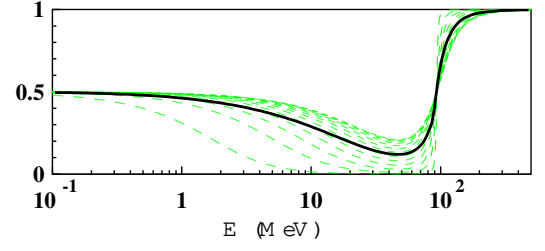


FIG. 3: $(P_{e \rightarrow e})_{\text{adiabatic}}$ averaged over one year (solid) and at intervals between an equinox and a solstice (dashed).

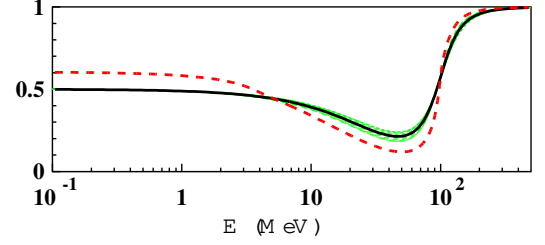


FIG. 4: $(P_{e \rightarrow e})_{\text{adiabatic}}$ for some modified models.

combination of effects produces ripples in the binned flux near the equinoxes, which might be detected in detailed experimental analyses of existing or future data.

Although detection of the semiannual variation would represent a definite positive signal for Lorentz violation, its absence cannot serve to eliminate this type of model. Simple modifications of the model exist that exhibit similar overall behavior for solar and atmospheric neutrinos but have only a small semiannual variation. As an illustration, consider the replacement of the coefficient $(a_L)_e^Z$ with a coefficient $(a_L)_e^T$ of half the size. This has the effect of replacing the solid and dashed curves of Fig. 3 with those shown in Fig. 4. The semiannual variations in this type of model lie below existing statistical sensitivities. Replacing also $(a_L)^Z$ with $(a_L)^T$ is another option, which removes all orientation dependence in the model. Another example of a small modification is a 10% admixture of $(a_L)_{ee}^T$, which raises the survival probability of 0.5 at low energies to about 0.6 without appreciably affecting other results. The ensuing survival probability in the adiabatic approximation is shown as the dotted line in Fig. 4. Other more complicated modifications that could be countenanced but that nonetheless retain the flavor of the simple model include allowing dependence on directions other than Z , or even introducing arbitrary coefficients $(a_L)_{ee}$, $(a_L)_e$, $(a_L)_e$, and $(c_L)_{ee}$, which yields a model with 21 degrees of freedom. More general possibilities also exist [7]. We conclude that positive signals for Lorentz violation could be obtained by detailed fitting of existing experimental data, but that it is challenging and perhaps even impossible at present to exclude the possibility that the observed neutrino oscillations are due to Lorentz and CPT violation rather than to mass differences.

The observations from long-baseline experiments are also compatible with the oscillation lengths in the simple two-coefficient model. For example, the oscillation length $2\pi = 31$ controls ν_e survival and is short enough to affect KamLAND [26]. An analysis incorporating the relative locations of the detector and the individual reactors would be of definite interest but lies outside our scope. Note, however, that the average ν_e survival probability is $P_{ee} = 1 - 2\sin^2 \theta_{12} \cos^2 \theta_{13} \approx 1/2$. A complete analysis is therefore likely to yield a reduced flux somewhat more than half the expected flux, in agreement with current data.

The new class of long-baseline accelerator-based experiments [27], planning searches for oscillations in ν_μ at GeV energy scales and distances of hundreds of kilometers, will be sensitive to sidereal variations. The model predicts ν_μ mixing with an experiment-dependent

pseudomass $m^2 = m_0^2 \cos^2 \theta$ because their beamlines are in different directions and so involve a different propagation angle θ . The energy dependence and transitions will be similar to the usual mass case.

Although the simple bicycle model reproduces most major features of observed neutrino behavior, it incorporates only a tiny fraction of the many possibilities allowed in the SME. More complexity could be introduced in performing a detailed fit to all existing data. Nonetheless, the model serves to illustrate a few key phenomena introduced by Lorentz violation. It also shows that the presence of Planck-scale Lorentz and CPT violation in nature could well first be revealed by a definitive signal in neutrino oscillations.

This work was supported in part by DOE grant DE-FG 02-91ER 40661 and by NASA grants NAG 8-1770 and NAG 3-2194.

-
- [1] For recent reviews of various approaches to Lorentz and CPT violation, see, for example, V.A. Kostelecky, ed., *CPT and Lorentz Symmetry II*, World Scientific, Singapore, 2002.
- [2] D. Colladay and V.A. Kostelecky, Phys. Rev. D 55, 6760 (1997); Phys. Rev. D 58, 116002 (1998); V.A. Kostelecky, Phys. Rev. D 69, 105009 (2004).
- [3] A comprehensive listing of experiments is given in K. Hagiwara et al., Phys. Rev. D 66, 010001 (2002), and updates at <http://pdg.lbl.gov>.
- [4] S.M. Carroll, G.B. Field, and R. Jackiw, Phys. Rev. D 41, 1231 (1990); V.A. Kostelecky and M. Mewes, Phys. Rev. Lett. 87, 251304 (2001).
- [5] V.A. Kostelecky and S. Samuel, Phys. Rev. D 39, 683 (1989); Phys. Rev. Lett. 63, 224 (1989); Phys. Rev. D 40, 1886 (1989). V.A. Kostelecky and R. Potting, Nucl. Phys. B 359, 545 (1991); Phys. Rev. D 51, 3923 (1995).
- [6] V.A. Kostelecky and R. Lehnert, Phys. Rev. D 63, 065008 (2001).
- [7] V.A. Kostelecky and M. Mewes, Phys. Rev. D 69, 016005 (2004).
- [8] Some of these are unobservable because they can be removed by suitable field redefinitions.
- [9] S. Coleman and S.L. Glashow, Phys. Rev. D 59, 116008 (1999).
- [10] V. Barger et al., Phys. Rev. Lett. 85, 5055 (2000).
- [11] J.N. Bahcall, V. Barger and D. Marfatia, Phys. Lett. B 534, 114 (2002).
- [12] G.L. Fogli et al., Phys. Rev. D 60, 053006 (1999); P. Lipari and M. Lusignoli, Phys. Rev. D 60, 013003 (1999); A. de Gouvêa, Phys. Rev. D 66, 076005 (2002).
- [13] V.A. Kostelecky and M. Mewes, Phys. Rev. D 66, 056005 (2002), Appendix C.
- [14] Super-Kamiokande Collaboration, S. Fukuda et al., Phys. Rev. Lett. 86, 5651 (2001); J. Yoo et al., hep-ex/0307070.
- [15] J. Lipa et al., Phys. Rev. Lett. 90, 060403 (2003); H. Muller et al., Phys. Rev. Lett. 91, 020401 (2003).
- [16] F. Cane et al., physics/0309070; D.F. Phillips et al., Phys. Rev. D 63, 111101 (2001); D. Bear et al., Phys. Rev. Lett. 85, 5038 (2000); R. Bluhm et al., Phys. Rev. Lett. 88, 090801 (2002); Phys. Rev. D 68, 125008 (2003); V.A. Kostelecky and C.D. Lane, Phys. Rev. D 60, 116010 (1999); J. Math. Phys. 40, 6245 (1999).
- [17] H. Dohrmelt et al., Phys. Rev. Lett. 83, 4694 (1999); R. Mittleman et al., Phys. Rev. Lett. 83, 2116 (1999); G. Gabrielse et al., Phys. Rev. Lett. 82, 3198 (1999); R. Bluhm et al., Phys. Rev. Lett. 82, 2254 (1999); Phys. Rev. Lett. 79, 1432 (1997); Phys. Rev. D 57, 3932 (1998).
- [18] B. Heckel, in Ref. [1]; L.-S. Hou, W.-T. Ni, and Y.-C. M. Li, Phys. Rev. Lett. 90, 201101 (2003); R. Bluhm and V.A. Kostelecky, Phys. Rev. Lett. 84, 1381 (2000).
- [19] V.W. Hughes et al., Phys. Rev. Lett. 87, 111804 (2001); R. Bluhm et al., Phys. Rev. Lett. 84, 1098 (2000).
- [20] KTeV Collaboration, H. Nguyen, in Ref. [1]; OPAL Collaboration, R. Ackersta et al., Z. Phys. C 76, 401 (1997); BELLE Collaboration, K. Abe et al., Phys. Rev. Lett. 86, 3228 (2001); BaBar Collaboration, B. Aubert et al., hep-ex/0303043; FOCUS Collaboration, J.M. Link et al., Phys. Lett. B 556, 7 (2003); V.A. Kostelecky, Phys. Rev. Lett. 80, 1818 (1998); Phys. Rev. D 61, 016002 (2000); Phys. Rev. D 64, 076001 (2001).
- [21] Note that existing constraints on lepton-sector Lorentz violation are irrelevant here because they are flavor diagonal and involve only part of the coefficients a_L . For specialized neutrino models with extra sterile neutrinos, these constraints may be important. See, for example, I. Mocioiu and M. Pospelov, Phys. Lett. B 537, 114 (2002).
- [22] L. Wolfenstein, Phys. Rev. D 17, 2369 (1978); S. Mikheev and A. Smirnov, Sov. J. Nucl. Phys. 42, 913 (1986).
- [23] An explicit example in a rotationally invariant model with a timelike coefficient $(a_L)^T$ is studied in Ref. [10].
- [24] LSND Collaboration, A. Aguilar et al., Phys. Rev. D 64, 112007 (2001).
- [25] MiniBooNE Collaboration, E. Church et al., Fermilab Report No. FERMILAB-P-0898, 1997.
- [26] KamLAND Collaboration, K. Eguchi et al., Phys. Rev. Lett. 90, 021802 (2003).
- [27] K2K Collaboration, M.H. Ahn et al., Phys. Rev. Lett. 90, 041801 (2003); MINOS Collaboration, Fermilab Report No. NuMI-L-337 (1998); ICARUS Collaboration, ICARUS-TM/2001-03 (2001); OPERA Collaboration, CERN/SPSC 2000-028 (2000).